Available online at www.sciencedirect.com
ScienceDirect
Matrix Biology 27 (2008) 96–106
MATRIX BIOLOGY
www.elsevier.com/locate/matbio

EMILINs interact with anthrax protective antigen and inhibit toxin action in vitro

Roberto Doliana [a,*,1], Veljko Veljkovic [b,1], Jelena Prljic [b], Nevena Veljkovic [b], Elisa De Lorenzo [a], Maurizio Mongiat [a], Giovanni Ligresti [a], Stefano Marastoni [a], Alfonso Colombatti [a,c,d]

[a] *Divisione di Oncologia Sperimentale 2, CRO-IRCCS, Aviano, Italy*
[b] *Laboratory for Multidisciplinary Research, Institute of Nuclear Sciences VINCA, Belgrade, Serbia*
[c] *Dipartimento di Scienze e Tecnologie Biomediche, Università di Udine, Udine, Italy*
[d] *MATI Center of Excellence, Università di Udine, 35100 Udine, Italy*

Received 13 June 2007; received in revised form 13 September 2007; accepted 26 September 2007

Abstract

The informational spectrum method (ISM) is a virtual spectroscopy method for the fast analysis of potential protein–protein relationships. By applying the ISM approach to the GeneBank protein database the vascular proteins EMILIN1 (*E*lastin *M*icrofibril *I*nterface *L*ocated Prote*IN*), EMILIN2, MMN1, and MMN2 were identified as additional anthrax PA antigen interacting molecules. This virtual molecular interaction was formally proven by solid phase assays using recombinant proteins. The interaction is independent of the presence of divalent cations and does not involve PA aspartic residue at 683, a critical residue in receptor binding. In fact, the D683A point mutation fully prevented the cell intoxication ability of PA in the presence of Lethal Factor, but it was fully ineffective on the binding of mutated PA to EMILIN1 and EMILIN2. The ISM approach also led to the identification of the potential interaction sites between PA and EMILINs. A PA mutant with a deletion at residue D425 and solid phase protein–protein interaction studies as well as deletion mutant of EMILIN2 confirmed the hypothesized interaction site. Our findings imply that the PA-cell surface receptor interaction is not likely to provide the full explanation for the vascular lesions and prominent hemorrhages that follow *Bacillus anthracis* infection and spreading and call into play vascular associated proteins such as EMILINs as potential inhibitory proteins.

Keywords: Informational spectrum method; Protective antigen; *Bacillus anthracis* (anthrax); EMILIN1; EMILIN2

1. Introduction

Bacillus anthracis is a gram-positive, spore-forming bacterium that causes anthrax in humans and animals. Anthrax toxin, the key virulence factor for *B. anthracis*, is composed of two separate A–B toxins, the edema factor (EF) or lethal factor (LF) catalytic A moieties and a shared binding B moiety, protective antigen (PA) that facilitates entry of the toxin into cells. EF is a Ca^{+}- and calmodulin-dependent adenylate cyclase (Leppla, 1982) and LF is a Zn^{+} metalloproteinase that cleaves several MAPK kinases (Vitale et al., 1998; Bernardi et al., 2000; Duesbery et al., 1998). However, to display full activity the initial step in the action of the toxin is the binding of protective antigen (PA) to a cell surface receptor. Binding is followed by cleavage of the full-length 83-kDa form of PA, resulting in removal of a 20-kDa fragment from the N terminus (Molloy et al., 1992). The cleavage generates a 63 kD PA that assemblies into a heptameric oligomer (Milne et al., 1994) and also provides binding sites for EF and/or LF (Mogridge et al., 2002).

The PA protein is subdivided into four domains based on its crystal structure, and the different domains exert distinct functions based on mutational and biochemical analyses

* Corresponding author. Divisione di Oncologia Sperimentale, Centro di Riferimento Oncologico, 33081 Aviano, Italy. Tel.: +39 0434 659 757; fax: +39 0434 659 428.
E-mail address: rdoliana@cro.it (R. Doliana).
[1] R.D. and V.V. contributed equally to this work.

0945-053X/$ - see front matter © 2007 Elsevier B.V./International Society of Matrix Biology. All rights reserved.
doi:10.1016/j.matbio.2007.09.008

(Scobie and Young, 2005). Domain 1 (residues 1–258) contains the hydrophobic portion which is exposed following furin cleavage to allow EF and LF to bind (Scobie et al., 2003). Domain 2 (residues 259–487) is involved in oligomerization and membrane channel formation through which the LF and EF enter the cytosol (Scobie and Young, 2005; Abrami et al., 2005). Domain 3 (residues 488–595) is required for oligomerization. Domain 4 (residues 596–735) is necessary for binding to cellular receptor(s). Mutational analysis studies and the use of neutralizing monoclonal antibodies localized the residues necessary for binding to receptor in and near the small loop of domain 4 (amino acids 679–693) and suggested that residues essential for binding were in that region (Rosovitz et al., 2003). Cell binding and toxicity assays implicated D683 as a critical residue in receptor binding (Abrami et al., 2003).

Two PA receptors have been identified in human cells: anthrax toxin receptor/tumor endothelial marker 8 (ATR/TEM8) (Bradley et al., 2001) and capillary morphogenesis protein 2 (CMG2) (Scobie et al., 2003). A murine ortholog of ATR/TEM-8 also has been reported (Carson-Walter et al., 2001). PA receptors consist of an extracellular domain, a membrane-spanning region, and a cytoplasmic tail. ATR/TEM8 and CMG2 proteins share 60% identity within their VWA domains, including a perfectly conserved metal ion-dependent adhesion site (MIDAS) motif (Mogridge et al., 2002; Scobie et al., 2003) that is involved in ligand interaction (Lee et al., 1995). The VWA domain fold is found in many cell adhesion proteins and promotes protein–protein interactions (Colombatti and Bonaldo, 1991; Whittaker and Hynes, 2002). This finding is consistent with an interaction between the carboxyl group of D683 of PA and the metal coordination site of the anthrax receptors, ATR/TEM8 and CMG2. Preservation of the MIDAS motif is required for ATR/TEM8 binding to PA. Soluble, recombinant VWA domains from ATR/TEM8 and CMG2 can inhibit anthrax intoxication of cultured cells (Milne et al., 1994; Abrami et al., 2005).

The informational spectrum method (ISM), a virtual spectroscopy method represents a promising approach for a fast and simple structure analysis of proteins and their functionally important domains (Veljkovic and Metlas, 1998; Pham 2006). This approach has been used successfully several times as a starting point to identify protein interactions by ourselves and others groups (several examples are reported in Parbhane et al., 2000; Shepherd et al., 2003; Krishnan et al., 2004; Wen et al., 2005; Sinkala, 2006). By applying the ISM to the analysis of the whole array of human proteins present in the GeneBank database we identified EMILIN1 (*E*lastin *M*icrofibril *I*nterface *L*ocated Prote*IN*) (Doliana et al., 1999) as well as other members of this family of extracellular matrix (ECM) proteins as novel and additional PA-binding sites. Specific interactions of domain 2 residues of PA with these proteins in vitro and the inhibition of cell cytotoxicity by the LF-PA complex in the presence of EMILIN1, suggests that the interpretation of the interplay between *B. anthracis* and cell membrane receptors in determining severe clinico-pathological consequences should take into account also the interactions with EMILIN family members.

2. Results

2.1. Proof of principle for ISM

Blocking the interaction between PA and its receptor represents the key step in the neutralization of the anthrax toxin function. For this reason, the identification of the regions of PA and ATR/TEM-8 participating in their interaction

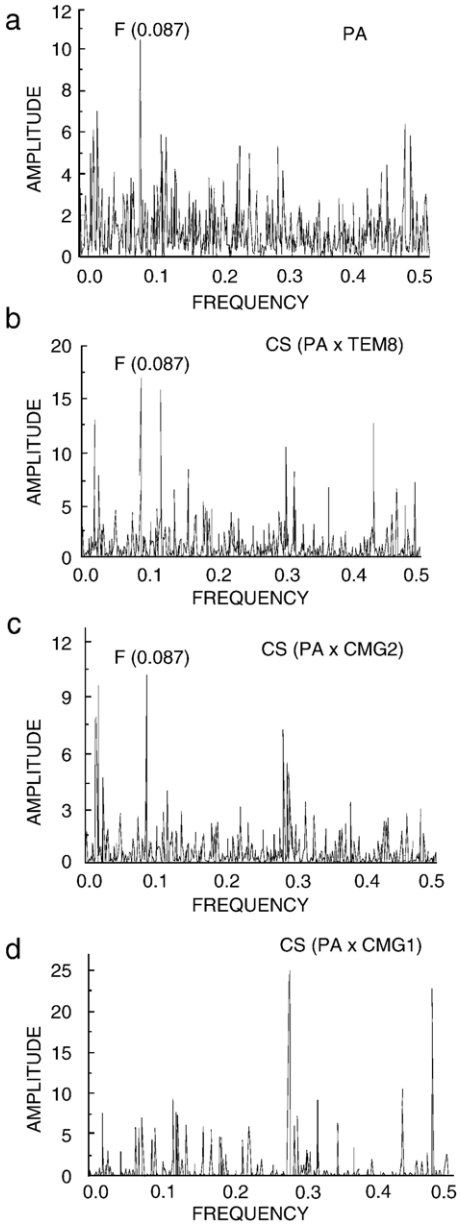

Fig. 1. Informational spectrum of PA and its receptors. (a) Informational spectrum (IS) of protective antigen (PA) and its receptor. (b) Cross-spectrum (CS) between PA and ART/TEM-8; (c) CS between PA and CMG2; and (d) CS between PA and CMG1. For each spectrum the abscissa represents the frequencies from the Fourier transform of the sequence of electron-ion interaction potential corresponding to the amino-acid sequence of the protein. The lowest frequency is 0.0 and the highest is 0.5. The ordinate represents amplitudes, in arbitrary units, corresponding to each frequency component in the spectrum.

represented an important step in developing a vaccine for an effective therapy against *B. anthracis* (Bradley et al., 2001).

According to the IS concept (Veljkovic and Cosic, 1987; Lazovic, 1996), the IS spectra of interacting proteins share common frequency component(s). To identify this important informational characteristic determining the interaction between PA and anthrax receptors ATR/TEM8 and CMG2, the ISM analysis of these proteins has been performed. In Fig. 1a, b and c are presented the individual informational spectrum (IS) of PA, cross-spectra (CS) between PA and ATR/TEM8, and CS between PA and CMG2, respectively. As can be seen from Fig. 1a, the dominant peak in IS of PA molecule corresponds to the frequency $F(0.087)$. It means that this frequency component represents dominant information encoded by primary structure of PA. The dominant peaks in CS between PA and ATR/TEM8, and CS between PA and CMG2 (Fig. 1b and c) also correspond to the frequency $F(0.087)$. These results imply that primary structures of these proteins encode the same information which is represented by IS frequency $F(0.087)$ and which determines PA/receptor interaction.

To verify whether the frequency component $F(0.087)$ represents information which is specific for PA/receptor interaction, the cross-spectral analysis between PA and the highly homologous non-receptor molecule CMG1 was performed. From results presented in Fig. 1d it is obvious that CS between PA and CMG1 does not contain any significant peak at the frequency $F(0.087)$. It means that primary structure of CMG1 does not contain information which allows ATR/TEM8 and CMG2 to interact with PA. This result is in accord with the lack of any receptor function of CMG1 for PA (Scobie et al., 2003).

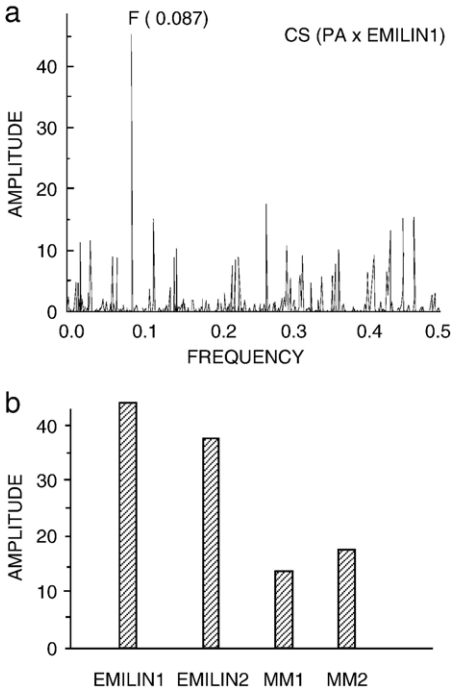

Fig. 2. Informational spectrum of EMILINs. (a) Cross-spectrum (CS) between PA and EMILIN1 The abscissa and ordinate are as described in Fig. 1. (b) Comparison between EMILINs. The amplitude at $F(0.087)$ for the different members of the EMILIN family is shown.

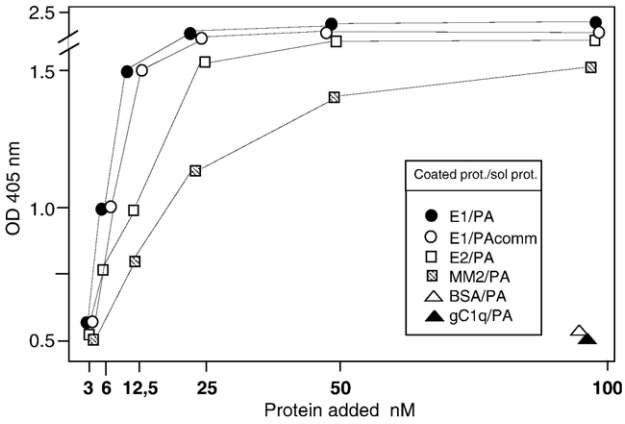

Fig. 3. Interaction between PA and EMILINs. Solid phase binding assays. Variable amounts of recombinant proteins were coated to the plastic surface of multi-well plates and incubated with PA at 50 nM fixed concentration. The data are the mean of triplicate assays.

2.2. Identification of additional ligand partners of PA by IS frequency

In order to identify new potential PA interactors the GeneBank was screened aiming at those proteins which are most compatible with PA in terms of information represented by frequency $F(0.087)$. By this computer assisted screening proteins with highest amplitude value and S/N ratio at the frequency $F(0.087)$ in CIS with PA have been selected as candidate interactors. Among these proteins EMILIN1 has the highest values of amplitude (44.5) and S/N ratio (23.4) in CS with PA (Fig. 2a). Based on this bioinformatics criterion EMILIN1 has been selected as a most promising candidate for PA interactor. EMILIN1 has a very close homologous member, EMILIN2 (Doliana et al., 2001) and other proteins that have a similar domain structure and organization and high sequence similarity such as MMN1 (Hayward et al., 1995) and MMN2 (Christian et al., 2001). Thus, we determined the amplitude and signal-to-noise values at the frequency $F(0.087)$ for EMILIN2, MMN1 and MMN2 and found that, albeit at lower amplitude compared to EMILIN1, also EMILIN2, MMN1 and MMN2 (amplitude 36.8, 20.3, and 23.2, respectively) were compatible with being potential interactors with PA (Fig. 2b).

To determine experimentally whether PA and EMILINs could interact, recombinant proteins were assayed for binding in solid phase assays. In preliminary studies we determined that our recombinant PA was indistinguishable from commercially available PA and both showed that binding to EMILIN1 was saturable, with saturation at about 20.0 nM (Fig. 3). Consistently higher values were obtained when soluble PA was added to immobilized EMILIN1 rather than when soluble EMILIN1 was added to immobilized PA (data not shown). Binding of either EMILIN1 or PA to immobilized BSA or gC1q1 was negligible. Next, proteins were immobilized to the plastic substrate at either pH 7.2 in phosphate buffer or at pH 9.6 in carbonate buffer; while EMILIN2 had similar binding saturation curves irrespective of the pH used for the immobilization, binding of EMILIN1 was higher when the protein was plated at pH 7.2; however, under both conditions

saturation levels were equivalent (data not shown). The fact that for the binding to occur no divalent cations were included in the assay, raised the possibility that the PA does not interact with EMILINs via a MIDAS site as it occurs with the classical PA receptors (see below). The kinetics of the interaction indicated that after 45 min of incubation there was no further increase of binding, irrespective of the immobilized protein, suggesting that at 45 min all the potential protein–protein interactions had taken place (data not shown).

Next, PA was analyzed in a comparative solid phase ELISA assay using immobilized human EMILIN2 or murine MMN2 plated at variable concentrations in phosphate buffer, pH 7.2. Also these proteins displayed a dose-dependent binding to PA (Fig. 3). Compared to human EMILIN1 that reached a 50% binding at 6.0 nM, EMILIN2 reached about 50% binding at about 10.0 nM and murine MMN2 at about 15.0 nM. The finding that additional ligands such as EMILIN2 and MMN2 also bind PA expands the range and nature of proteins capable to interact with the *B. anthracis* PA protein that is fundamental for subsequent toxin activity within the cells.

2.3. Binding of EMILINs to PA is not dependent on D683

Two important features determine the interaction between PA and its cell surface receptors ATR/TEM-8 and CGM-2: the presence of divalent cations (Mn^{+} or Mg^{+}) and residue D683 that is by far the most critical for receptor binding and cell toxicity (Abrami et al., 2003; Santelli et al., 2004; Bradley et al., 2003; Singh et al., 2001), since it is a necessary residue for completing the coordination of the MIDAS metal by virtue of its carboxylate side chain. We have shown that EMILINs interacted very efficiently with PA even in the absence of divalent cations. Thus, we explored whether residue D683 was relevant also for this interaction. As expected there was no difference between wild type PA and D683A mutant: both EMILIN1 and EMILIN2 bound with the same efficiency irrespective of the ligand (Fig. 4a). The fact that binding did not require divalent cations and was not dependent upon D683 is not surprising since EMILINs have no VWA type domain that could correspond to the integrin-like recognition site on either ATR/TEM-8 or CGM-2.

2.4. EMILIN1 and EMILIN2 prevent PA toxic effects

The initial step in the action of *B. anthracis* is the binding of PA to a cell surface receptor. Receptor-bound PA is cleaved into two fragments by a furin family protease (Molloy et al., 1992). Dissociation of the smaller fragment allows the larger fragment, which remains receptor-bound, to self-associate into ring-shaped heptamers via domain 2 of PA. The proteolytic cleavage of receptor-bound PA is a fundamental prerequisite not only for PA self-assembly and LF and EF binding but also for the subsequent step of endocytic internalization. Having shown that

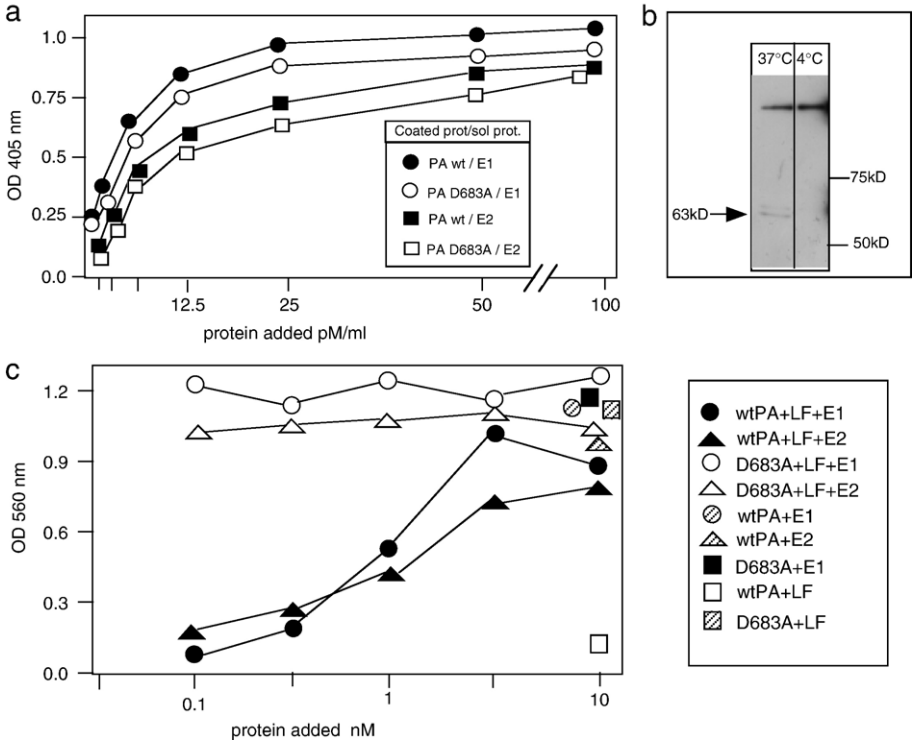

Fig. 4. Inhibition of PA-EF cell intoxication by EMILIN1. (a) Solid phase binding assays showing that recombinant wild type PA (closed circles) or D683A mutant PA (open circles), coated to the plastic surface of multi-well plates at fixed concentrations (range 20–100 nM) and incubated with variable amounts of EMILIN1 or EMILIN2 displayed equivalent binding. The assay was performed in triplicate; (b) Cleavage of PA. J774 cells were incubated for 20 min at different T with PA and at the end of incubation cells were lysed, separated on SDS-PAGE, transferred to nitrocellulose filters and incubated with 6His tag specific antibodies. As expected at 37 °C PA is partially cleaved in a fragment of 63 kD; (c) Cell intoxication. J774 cells were incubated with 10^{-7} M wild type PA or D683A mutant PA and 10^{-9} M LT in the presence of increasing amounts of EMILIN1 (0.1–10 nM). Cell viability after intoxication was then measured at 24 h by using an MTT assay. EMILIN1 and PA were pre-incubated for half an hour at room temperature before addition to the cells. The assay was performed in triplicate.

EMILIN1 binds to PA and that this interaction is not involving residue D683 of PA, we asked whether this interaction might affect the interaction of PA with its receptor(s). J774 cells plated 48 h before were treated with PA (10^{-7} and 10^{-8} M) pre-incubated with increasing amounts of EMILIN1 or EMILIN2 in the presence or in the absence of a constant amount of LF. First, PA bound to J774 cells was rapidly cleaved to PA63 (Fig. 4b) indicating that functional processing had taken place. Then, cell viability after intoxication was measured by an MTT assay (Fig. 4c). In the presence of PA and LF nearly all cells were killed; however, EMILIN1 and EMILIN2 were both able to competitively inhibit cell killing with 50% inhibition attained at about 2–3 pM. As expected D683A PA was unable to kill any target cell (Fig. 4c).

2.5. Identification of the PA and EMILINs interacting regions

In order to localize the binding site(s) for PA on EMILIN2, we took advantage of recombinant polypeptides of human EMILIN2, produced within the framework of a different study (Mongiat et al., 2007) and shown to correspond to the expected molecular weights (Fig. 5b, left panel). Despite the fact that Δ1

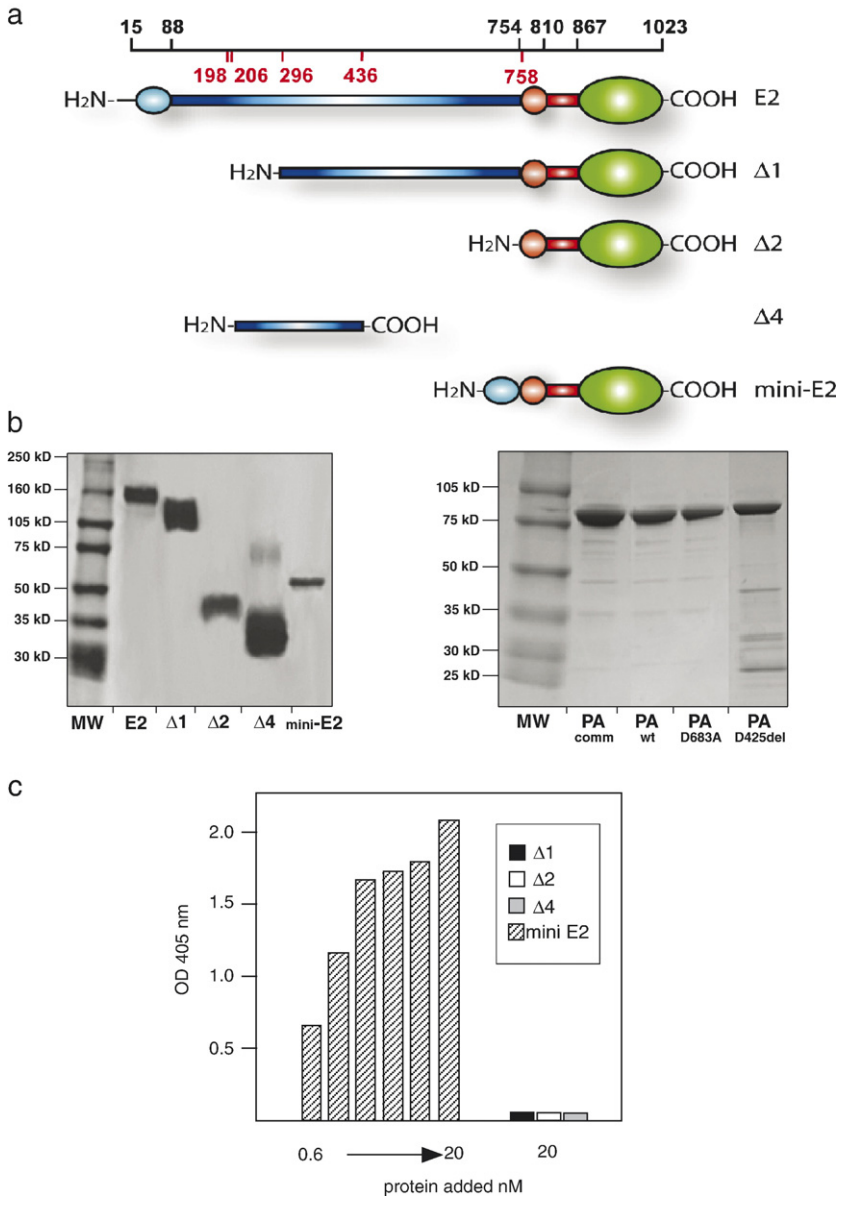

Fig. 5. Mapping of EMILINs region interacting with PA. (a) Top: scheme of EMILIN2 and deletion mutants. EMI domain, *light blue*; coiled-coil region, *blue*; proline-rich region, *orange*; collagen stalk, *red*; g-C1q2 domain, *green*. *Black figures* indicate the domain amino-acid residues position; *red figures* indicate the deletions positions; bottom: SDS-PAGE of the recombinant products. (b) SDS-PAGE of the EMILIN2 recombinant constructs (left) and of all the PA constructs used in this work (right). (c) Binding of deletion constructs of human EMILIN2, Δ1, Δ2, Δ4, and mini-E2 to PA. Recombinant PA coated to the plastic surface of multi-well plates at 20 nM was incubated with variable amounts of the various recombinant proteins (for simplicity only the data obtained with the maximal amount used of Δ1, Δ2, and Δ4 are indicated). The assay was performed in triplicate.

(residues 296–1023 of the mature protein) and Δ2 (residues 758–1023) contain the gC1q domain and were able to promote cell adhesion (unpublished) and Δ4 (residues 198–436) interacted with the death receptor DR4 (M. Mongiat et al., 2007) and are thus functionally active, none of these polypeptides bound PA (Fig. 5). This suggested that the binding site for PA was localized within the first 200 residues of EMILIN2. Next, a construct comprising the N- (residues 15–88) fused to the C-terminal (residues 758–1023) region (mini-E2) was assayed and found to provide a very good binding partner for PA. Thus, the interacting site on EMILIN2 lies within the 15–88 residues, a segment corresponding to the EMI domain and, since EMILIN1 and EMILIN2 share a high sequence homology in this region (Doliana et al., 2000), it is likely that also EMILIN1 interacts with PA through the same domain.

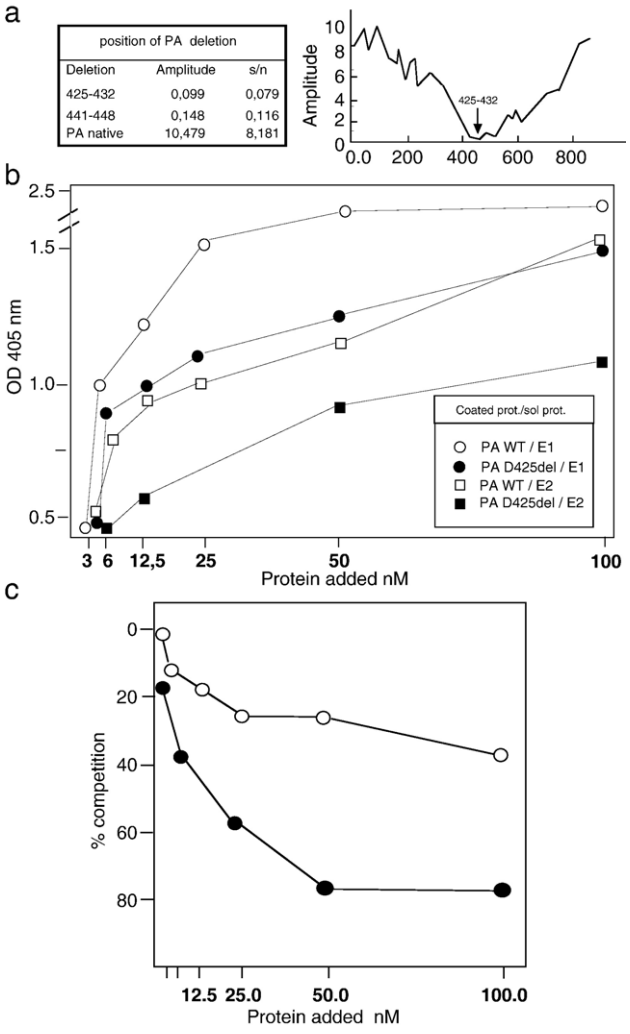

Fig. 6. Identification of the region in PA interacting with EMILINs. (a) ISM analysis of in silico deletions of PA. Systematic scanning of seven residues long deletion of PA shows that deletion of aa 425–432 and aa 441–448 cause a dramatic decrease of CS amplitude at frequency *F*(0.087); (b) Solid phase binding assays. Recombinant PAs was coated to the plastic surface of multi-well plates at fixed concentration of 50 pM/ml and incubated with variable amounts of EMILIN1 or EMILIN2. The data are the mean of triplicate assays. (c) Competition of the binding of soluble EMILIN1(1 nM) to wtPA coated at 0.1 μg/ml. Competition was with wild type (*closed circles*) or del425 PA (*open circles*). del425 is unable to compete with wtPA for the binding of EMILIN1. The assay was performed in triplicate.

Then, the ISM method again was applied in order to identify the PA domain which is essential for information corresponding to the IS frequency *F*(0.087). For this purpose the amplitude of PA at the frequency component *F*(0.087) was measured after applying theoretical deletions of different length to the primary sequence (window was 1 to 20 residues). We found that deletion of 7 residues represents the minimal length of deletion which decrease amplitude on the frequency *F*(0.087) below the noise. As shown in Fig. 6a the amplitude dropped at nearly zero values with deletions encompassing residues 425–448. Within this region important residues are present that upon mutation result in variants of PA that disrupt the function of the *B. anthracis* in vitro (Sellman et al., 2001; Ahuja et al., 2003). In particular, deletion of D425 or F427 (see Fig. 5b, right panel) yielded dominant negative mutants of PA that bind to cell surface receptors and are proteolitically cleaved but are unable to form pore and mediate translocation of LF/EF, resulting in the most potent inhibitors that neutralize the activity of the *B. anthracis* toxins (Ahuja et al., 2003). We thus deleted residue aspartic acid 425 (D425del) and assayed binding of EMILIN1 or EMILIN2 to wtPA or D425del. As depicted in Fig. 6b binding of either EMILIN1 or EMILIN2 to D425del was lower than binding to wtPA. To further analyze this interaction a competition assay in which wtPA was plated and binding of EMILIN1 was inhibited by soluble wtPA or D425del mutant was performed. As shown in Fig. 6c, D425del was poorly capable of competing the EMILIN1/wtPA interaction compared to the wild type PA, suggesting that residue D425 in domain 2 of PA plays also an important role in the interaction with EMILIN1 and likely EMILIN2.

3. Discussion

PA is a central component of *B. anthracis* toxin, serving as a cellular binding moiety and a delivery vehicle for translocation of EF and LF into the cytosol of cells. Therefore, the interaction between PA and the target cell has been a central issue in studies of *B. anthracis* intoxication. These analyses revealed that PA not only rapidly binds to ART/TEM-8 and/or CGM-2 cell surface receptors but it also is rapidly cleaved by a furin protease to a 63 kD polypeptide within 5 min (Molloy et al., 1992).

However, despite the significant breakthrough made by the discovery of the anthrax receptors, many important questions concerning the interaction between this pathogen and its tissue targets remain open. This is particularly relevant for the vascular lesions representing the basis of the prominent hemorrhages of the human inhalational anthrax (Mayer et al., 2001). In fact, while it is well established that inhaled spores are phagocytosed by alveolar macrophages and then transported by these cells to the pulmonary hilar and mediastinal lymph nodes, the vascular lesions that likely result from direct insults to the host cells, i.e. endothelial and smooth muscle, suggest the existence of other anthrax receptor/binding sites which could be involved in multiple interactions with vascular tissues.

The present study has identified a new series of PA-binding proteins expressed predominantly in the vasculature ECM. In fact, both EMILIN1 and EMILIN2 (Colombatti et al., 1985; Braghetta et al., 2004) as well as MMN1 (Hayward et al., 1995), MMN2 (Christian et al., 2001; Doliana et al., unpublished) are distributed within blood vessel walls. The potential interaction between PA and EMILIN1, EMILIN2, MMN1, and MMN2 was presumed on the basis of the ISM and cross-spectral analyses of the human proteins present in the GeneBank database. This method has proven effective in identifying potential protein–protein domain interactions in several examples such as gp120 (Veljkovic and Metlas, 1998), β-globin (Arrigo et al., 2002), and YB-1 (Huang et al., 2005). With this approach one major IS frequency component $F(0.087)$ with maximal amplitude was found that suggested the existence of regions of direct interaction. EMILIN1 is apparently the preferred binding partner: in fact, the amplitude values for the interaction between PA and EMILIN1 were higher than those with the other binding partners including CGM2. This virtual spectroscopic interaction was validated by direct interaction between PA and EMILIN1, EMILIN2, and MMN2 in vitro. In addition, both EMILIN1 and EMILIN2 were able to competitively inhibit J774 cell intoxication in the presence of PA and LF, thus suggesting that these new interactors might play a functional role during *B. anthracis* infection.

Binding of PA to ATR/TEM8 or CGM2 is known to involve the VWA domains of either receptor and requires both divalent cations and an aspartic residue. Although the aspartic acid in the motif is fundamental for ligand binding (Santelli et al., 2004; Bradley et al., 2003; Singh et al., 2001) and approximately 46% of all VWA domains have a perfectly conserved metal ion-dependent adhesion site (MIDAS) motif (DXSXS... T... D, where X is any amino acid), which is often involved in ligand binding (Lee et al., 1995). The interaction between PA and EMILIN1, EMILIN2, or MMN2 was independent of divalent cations and none of the EMILIN protein family members has a VWA domain nor a MIDAS motif; thus, interaction had to involve different binding sites. Accordingly, while a D683A mutant was unable to intoxicate and kill appropriate target cells in the presence of LF, it was equally efficient in supporting EMILIN1 and EMILIN2 binding as the wild type PA polypeptide. This result is in accord with previous studies in which the substitution of residue D683 impaired its ability to bind and intoxicate cells and prevented its binding to the soluble form of ATR/TEM8 (Santelli et al., 2004; Singh et al., 2001).

The binding regions on EMILINs and PA were then identified by a three-step approach. First, deletion mutants of EMILIN2 and a mini-E2 construct comprising the N- and C-terminal regions limited the interacting part to the N-terminal EMI domain, a 80 residues long domain with a conserved pattern of seven cystein. Little is known about this domain but recently it has been shown in mouse model that EMILIN1 acts through the EMI domain in regulating pro TGF-beta processing, with important consequences on blood pressure homeostasis (Zacchigna et al., 2006). Second, ISM on in silico deleted PA molecules suggested that a region around residue 400 might be involved. Third, a deletion mutant of PA (del425) bound to EMILIN1 and EMILIN2 with very poor efficiency and was unable to compete with wtPA for the binding to EMILIN1. Residue D425 is important in mediating EF/LF toxicity and its deletion results in a variant of PA which assembles to form non-functional complexes leading to a complete inhibition of the channel forming ability of PA (Ahuja et al., 2003). The present finding indicating that EMILINs interact with the same area of PA suggests that they might prevent or negatively affect *B. anthracis* infections by binding to PA and blocking its pore-forming function as shown for newly developed drugs (Karginov et al., 2005).

The formal demonstration that PA interacts with EMILIN1, EMILIN2, and MMN2 in vitro deserves some considerations. One possibility is that, being these polypeptides particularly expressed at and underneath the endothelium and in vascular smooth muscle, they could represent elective sites for *B. anthracis* tissue deposition. Direct vascular lesions are responsible for the prominent focal hemorrhages for human inhalational anthrax (Grinberg et al., 2001) and for the injuries of aorta in similarly affected patients (Holty et al., 2006; Mayer et al., 2001). The finding that EMILIN1 but also the other members of the family are particularly present in some vascular tissues suggests that they could function as potential "decoy receptor/binding proteins" hence reducing the number of bacteria able to bind to cell surfaces and intoxicate target cells.

Thus, EMILINs along with the LDL receptor-related protein LRP6 (Wei et al., 2006), whose crucial role in endocytosis of anthrax has been however recently confuted by Young et al. (2007), represent additional potential targets and/or proteins useful for countermeasures against *B. anthracis* toxin lethality.

4. Experimental procedures

All analyzed protein sequences were taken from the GeneBank database (release 136.0, August 2003). For structure–function analysis of proteins an in house computer program based on ISM was used (public access at web site http://cmdwave.bii.a-star.edu.sg/). Complete description and details of the ISM have been published elsewhere (Veljkovic and Cosic, 1987; Lazovic, 1996), and here only a brief description of this approach will be given.

4.1. Informational spectrum method

The ISM technique is based on a model that assigns to each amino acid a defined parameter describing a physico-chemical property involved in the biological activity of the protein and corresponding to electron-ion interaction potential (EIIP) (Veljkovic and Slavic, 1972). Thus, these values determine the electronic properties of amino acids responsible for their intermolecular interactions (Veljkovic, 1980). The obtained numerical sequence, representing the primary structure of a protein, is then subjected to a discrete Fourier transformation which is defined as follows:

$$X(n) = \Sigma x(m) e^{-j(2/N)nm}, \quad n = 1, 2, \ldots, N/2 \qquad (1)$$

where $x(m)$ is the m-th member of a given numerical series, N is the total number of points in this series, and $X(n)$ are discrete

Fourier transformation coefficients. These coefficients describe the amplitude, phase and frequency of sinusoids, which comprised the original signal. The absolute value of complex discrete Fourier transformation defines the amplitude spectrum and the phase spectrum. The complete information about the original sequence is contained in both spectral functions. However, in the case of protein analysis, relevant information is presented in energy density spectrum (Pham, 2006), which is defined as follows:

$$S(n) = X(n)X^*(n) = |X(n)|^2, \quad n = 1, 2, \ldots, N/2. \tag{2}$$

In this way, sequences are analyzed as discrete signals. It is assumed that their points are equidistant with the distance $d=1$. The maximal frequency in a spectrum defined in this way is $F=1/2d=0.5$. The frequency range is independent of the total number of points in the sequence. The total number of points in a sequence influences only the resolution of the spectrum. The resolution of the N-point sequence is $1/n$. The n-th point in the spectral function corresponds to a frequency $f(n)=nf=n/N$. Thus, the initial information defined by the sequence of amino acids now is presented in the form of the informational spectrum (IS), representing the series of frequencies and their amplitudes.

The IS frequencies correspond to the distribution of structural motifs with defined physico-chemical characteristics responsible for the biological function of a protein. When comparing proteins which share the same biological or biochemical function, the ISM technique allows detection of code/frequency pairs which are specific for their common biological properties, or which correlate with their specific interaction. This common informational characteristics of sequences are determined by cross-spectrum (CS). A measure of similarity for each peak is a signal-to-noise ratio (S/N), which represents a ratio between signal intensity at one particular frequency and the main value of the whole spectrum. If one calculates a CIS for a group of proteins having different primary structures, and finds strictly defined peak frequencies, it means that the analyzed proteins participate in mutual interaction or have a common biological function.

4.2. Preparation of recombinant proteins — human EMILIN1

293 cells, constitutively expressing the EBNA-1 protein (293-EBNA), were transfected with the constructs for human EMILIN1 and the protein purified as previously described (Mongiat et al., 2000). *Human EMILIN2*: EMILIN2 cDNA (Doliana et al., 2001) was retrotranscribed from total human kidney RNA and cloned into pCEP-Pu mammalian vector containing the sequence of the BM40 signal peptide to allow the secretion of the protein outside the cell. The following oligonucleotides were used: forward, 5′-CTAGCTAGCAGGCCCGCAGCCCGGG-3′ containing an NheI site and reverse, 5′-CGGGATCCTTAATGGTGATGGTGATGATGGAGGTGGGAAAGGAA-3′, containing a BamHI site and a 6His-tag sequence. *Δ1, Δ2 and Δ4*. EMILIN2 deletion constructs Δ1 and Δ2 were generated using EcoRI and NarI restriction enzymes. Δ4 cDNA was amplified using the full-length construct as a template with the following oligonucleotides, forward: 5′-CTAGCTAGCAGGCCCGCAGCCCGGGTAT-3′ and reverse: 5′-CGGGATCCTTAAGGCT TGGGGTGCTGGCT-3′ containing an NheI site in the forward oligonucleotide and a BamHI site in the reverse. *EMILIN2 minigene (mini-E2)*: the EMILIN2 minigene was produced cutting the pCEPu-EMILIN2 construct with the NheI polylinker enzyme and the natural occurring NarI site located in position 2370 of the coding sequence just up to the prolin rich region, and inserting an NheI/NarI-PCR product spanning the EMI domain. The resulting construct includes the N-terminal (residues 1–108) fused to the C-terminal region of EMILIN2 (residues 758–1023). *Murine MMN2*: a pCEP-Pu-FLAG eukaryotic expression vector was prepared by an in-frame insertion of a linker coding for the so called FLAG tag (DYKDDDDK) between NheI and XhoI sites. The cDNA sequences coding for the mature forms of murine MMN2 was excised from an existing full-length constructs provided by Prof. G.M. Bressan by sequential XbaI digestion, blunting, and XhoI digestion. The insert was gel purified and cloned in the pCEP-Pu-flag vector by using the common XhoI site and a blunted BamHI site.

All the resulting constructs are intended to direct expression of significative amount of a protein with a signal peptide for efficient secretion and a N-terminal FLAG peptide or 6His-tag for easy purification. The constructs were transfected in E293 cells, and the clones resistant to the selective antibiotic puromycin analyzed for protein expression by immunoblotting with an anti FLAG (Sigma) or an anti 6His (Clonetech) antibody. Positive clones were massively expanded and the pooled growth medium incubated with an agarose-linked anti FLAG antibody (Sigma) or an anti 6His (Clonetech) antibody. The resins were washed and eluted by FLAG peptide competition or elution with 150 mM Imidazole in 0.1 mM Na-phosphate, pH 7.0. *Protective antigen*: Native PA purified from *B. anthracis* was purchased from List Biological Laboratories, Inc, or produced as bacterial recombinant protein. Briefly, the sequence corresponding to the mature PA protein was amplified by RT/PCR using the following oligonucleotides: sense, 5′-ccggatccGAAGTTAAACAGGAGAAC3′; antisense, 5′-GGCTATGAGATAGGATAAggtac cgg, where the lower cases correspond to BamHI and KpnI appended tails, respectively. The amplified product was then restricted and ligated in frame in the 6His-tagged pQE30 expression vector (Qiaexpress Qiagen, GmbH). As PA is mainly localized in inclusion bodies, the expressed protein was purified under denaturing conditions and refolded following a protocol yielding active protein as in Gupta et al. (1999). The fractions eluted from the NiNTA (Quiagen GmbH) were analyzed on SDS-PAGE and those containing the protein were pooled and dialyzed against Tris–HCl, 10 mM pH 8.0 and EDTA 5 mM buffer. The PA was stored in aliquots at −80 °C. *Lethal factor*: fusion proteins of glutathione S-transferase (GST) with LF (GST::LF), a gift of Dr. Gaetano Vitale, were expressed in *E. coli* strain BL21 DE3 pUBS 520 (Schenk et al., 1995) and purified by affinity chromatography on GSH-Sepharose beads (Pharmacia), and by anion-exchange and size-exclusion chromatography as described (Hayward et al., 1995). All proteins were more than 90% pure as judged by SDS/PAGE and Coomassie Blue staining.

4.3. In vitro site-directed mutagenesis

QuickChange XL mutagenesis was performed according to manufacturer's instruction (Stratagene) to introduce the D683A mutations into the full-length PA. The mutant was generated by PCR amplification using as template the pQE-PA wild type and as primers oligonucleotides 5′-GATTTTAAAAAATA-TAATGCTAAATTACCG-3′ and its reverse complement. D425del was produced by PCR directed mutagenesis, cutting the pQE-PA wild type in 3′ with the polylinker restriction enzyme KpnI and in 5′ with the natural occurring NarI site lying just 24 bases up to the D683 and inserting a PCR product obtained with a NarI-5′ primer carrying the desired mutation 5′-TTGGCGCCAATCGCATTAAATGCACAA GATTT-CAGTTCTACTC 3′- and a KpnI-3′primer 5′-ATCTTTTC-TAAAAAAGGCTATGAGA TAGGATAAGGTACCGG-3′. Production and purification of D683A and D425del mutants was as described above for wild type PA. All the constructs used in the present study have been sequenced to check for any PCR-introduced errors and found to correspond to the correct sequence.

4.4. Protein interaction studies

For solid phase binding assays 10 μg/ml of human EMILIN1 and EMILIN2, Δ1, Δ2, Δ4, mini-E2 and murine MM2 stored at −80 °C or freshly expressed and purified PA in 0.1 M carbonate buffer, pH 9.6, or phosphate buffer, pH 7,2 were coated onto 96-multi-well plates (Greiner) for 16 h at 4 °C. After 3 washes with PBS without Ca^{+} and Mg^{+}, the non-specific binding sites were blocked with 2% (w/v) BSA in PBS for 2 h at 4 °C. The coated wells were then incubated with serial dilutions of the respective ligand for 45 min at room T, washed three times, and incubated with specific antibodies: rabbit polyclonal antiserum against EMILIN1 (diluted 1:1000) to detect EMILIN1 and gC1q1 (Doliana et al., 1999); a mAb anti FLAG (Sigma) to detect MM2, mAb 828B3 against gC1q2 of human EMILIN2 to detect EMILIN2, Δ1 and Δ2; a polyclonal mouse antiserum against Δ4; and a mAb against 6-His tag (Clontech) to detect PA and mini-E2. After 1 h the bound proteins were subjected to three washes, the wells were incubated with peroxidase-conjugated goat or rabbit immunoglobulins for 1 h and washed again. Bound ligands were detected by a color reaction for 3–5 min with the addition of ABTS and 0.01% H_2O_2. Color yields were determined at OD_{405} nm.

4.5. Assay of PA-binding to cells

PA binding to cells was assessed at both 37 and 4 °C. Cells were grown in 24-well plates to confluence. Cells were incubated with 1 μg/ml PA for 1 h and then washed five times with Hanks' balanced salt solution (HBSS) (Biofluids, Rockville, MD). In measurements of PA processing, the cells were lysed in 100 μl of lysis buffer (50 mM Tris–HCl, pH 7.4, 1% Nonidet P-40, 0.25% sodium deoxycholate, 150 mM NaCl, 1 mM EDTA, 1 mM phenylmethylsulfonyl fluoride, 1 μg/ml each of aprotinin, leupeptin, and pepstatin). The cell lysates were subjected to SDS-PAGE or native-PAGE using 4–20% Tris–glycine gradient gels (NOVEX, San Diego). Prior to loading, the cell lysates were boiled for 5 min in 1× SDS sample buffer (50 mM Tris–HCl, pH 6.8, 2% SDS, 100 mM dithiothreitol, 0.01% bromphenol blue, 6% glycerol) for SDS-PAGE. The proteins were then transferred to nitrocellulose membranes, followed by Western blotting with a mAb specific for the 6-His tag and PA was visualized by chemiluminescence using the ECL Western Blotting Detection Reagents (Amersham Biosciences).

4.6. Cell culture and cytotoxicity assay

The biological activity of the PA was determined by a cytotoxicity assay. Cytotoxicity was determined by the percentage of cell viability after incubation with LF (a kind gift from Dr. Gaetano Vitale), PA and h-EMILIN1 using MTT dye. LF is correctly folded and is fully active as previously shown (Vitale et al., 1998; Bernardi et al., 2000). The macrophage-like cell line J774 was maintained in DMEM medium containing 10% heat-inactivated FCS. The cell suspension was plated at 200 μl/well in 96-well flat bottom plates (30,000 cells/well), and cells were allowed to adhere by incubation at 37 °C for 16 h (95% humidity and 5%CO_2). The next day medium and detached cells were removed by gentle aspiration and replaced (200 μl/well) with DMEM containing 10^{-9} M LF and varying concentrations of EMILIN1 pre-incubated with 10^{-7} M or 10^{-8} M purified PA (for half an hour at room temperature). The cells were allowed to grow at 37 °C in a humidified CO_2 incubator. All experiments were done in triplicates. The following day MTT dye dissolved in PBS (2.5 μg/ml), added to the cells to a final concentration of 0.5 μg/ml and the cells were incubated for 3 h at 37 °C to allow uptake and oxidation of the dye by viable cells. The medium was replaced by 200 μl of 0.5% (w/v) SDS, 25 mM HCl in 90% isopropyl alcohol, and vortexed to dissolve the precipitate. The absorption was read at 560 nm using a microplate reader (Labsystems Multiskan MS) from which the extent of cytotoxicity was determined.

Acknowledgements

This work was supported by grants from AIRC and Departmental funds (to A.C.). Dr. Gaetano Vitale (University of Udine, Italy) is greatly acknowledged for providing LF.

References

Ahuja, N., Kumar, P., Alam, S., Gupta, M., Bhatnagar, R., 2003. Deletion mutants of protective antigen that inhibit anthrax toxin both in vitro and in vivo. Biochem. Biophys. Res. Commun. 307 (3), 446–450.

Abrami, L., Liu, S., Cosson, P., Leppla, S.H., van der Goot, F.G., 2003. Anthrax toxin triggers endocytosis of its receptor via a lipid raft-mediated clathrin dependent process. J. Cell Biol. 160 (3), 321–328.

Abrami L., Reig N., van der Goot F.G., 2005. Anthrax toxin: the long and winding road that leads to the kill. Trends Microbiol. 2, 72–78. Review.

Arrigo, P., Ivaldi, G., Cardo, P.P., 2002. In silico determination of potential antisense targets for human beta-globin variants. In Silico Biol. 2, 143–150.

Bernardi, L., Vitale, G., Montecucco, C., Musacchio, A., 2000. Expression, crystallization and preliminary X-ray diffraction studies of recombinant

Bacillus anthracis lethal factor. Acta Crystallogr., D Biol. Crystallogr. 56 (Pt 11), 1449–1451.

Bradley, K.A., Mogridge, J., Mourez, M., Collier, R.J., Young, J.A., 2001. Identification of the cellular receptor for anthrax toxin. Nature 414 (6860), 225–229.

Bradley, K.A., Mogridge, J., Jonah, G., Rainey, A., Batty, S., Young, J.A., 2003. Binding of anthrax toxin to its receptor is similar to alpha integrin-ligand interactions. J. Biol. Chem. 278 (49), 49342–49347.

Braghetta, P., Ferrari, A., De Gemmis, P., Zanetti, M., Volpin, D., Bonaldo, P., Bressan, G.M., 2004. Overlapping, complementary and site-specific expression pattern of genes of the EMILIN/Multimerin family. Matrix Biol. (7), 549–556.

Carson-Walter, E.B., Watkins, D.N., Nanda, A., Vogelstein, B., Kinzler, K.W., Croix, B., 2001. Cell surface tumor endothelial markers are conserved in mice and humans. Cancer Res. 61 (18), 6649–6655.

Christian, S., Ahorn, H., Novatchkova, M., Garin-Chesa, P., Park, J.E., Weber, G., Eisenhaber, F., Rettig, W.J., Lenter, M.C., 2001. Molecular cloning and characterization of EndoGlyx-1, an EMILIN-like multisubunit glycoprotein of vascular endothelium. J. Biol. Chem. 276 (51), 48588–48595.

Colombatti, A., Bonaldo, P., 1991. The superfamily of proteins with von Willebrand factor type A-like domains: one theme common to components of extracellular matrix, hemostasis, cellular adhesion, and defense mechanisms. Blood 77, 2305–2315.

Colombatti, A., Bressan, G.M., Castellani, I., Volpin, D., 1985. Glycoprotein 115, a glycoprotein isolated from chick blood vessels, is widely distributed in connective tissue. J. Cell Biol. 100 (1), 18–26.

Doliana, R., Mongiat, M., Bucciotti, F., Giacomello, E., Deutzmann, R., Volpin, D., Bressan, G.M., Colombatti, A., 1999. EMILIN, a component of the elastic fiber and a new member of the C1q/TNF superfamily of proteins. J. Biol. Chem. 274, 16773–16781.

Doliana, R., Bot, S., Bonaldo, P., Colombatti, A., 2000. EMI, a novel cysteine-rich domain of EMILINs and other extracellular proteins, interacts with the gC1q domains and participates in multimerization. FEBS Lett. 484 (2), 164–168.

Doliana, R., Bot, S., Mungiguerra, G., Canton, A., Cilli, S.P., Colombatti, A., 2001. Isolation and characterization of EMILIN-2, a new component of the growing EMILINs family and a member of the EMI domain-containing superfamily. J. Biol. Chem. 276 (15), 2003–2011.

Duesbery, N.S., Webb, C.P., Leppla, S.H., Gordon, V.M., Klimpel, K.R., Copeland, T.D., Ahn, N.G., Oskarsson, M.K., Fukasawa, K., Paull, K.D., Vande Woude, G.F., 1998. Proteolytic inactivation of MAP–kinase–kinase by anthrax lethal factor. Science 280 (5364), 734–737.

Grinberg, L.M., Abramova, F.A., Yampolskaya, O.V., Walker, D.H., Smith, J.H., 2001. Quantitative pathology of inhalational anthrax I: quantitative microscopic findings. Mod. Path. (5), 482–495.

Gupta, P., Waheed, S.M., Bhatnagar, R., 1999. Expression and purification of the recombinant protective antigen of *Bacillus anthracis*. Protein Exp. Purif. 16, 369–376.

Hayward, C.P., Hassell, J.A., Denomme, G.A., Rachubinski, R.A., Brown, C., Kelton, J.G., 1995. The cDNA sequence of human endothelial cell multimerin. A unique protein with RGDS, coiled-coil, and epidermal growth factor–like domains and a carboxyl terminus similar to the globular domain of complement C1q and collagens type VIII and X. J. Biol. Chem. 270 (31), 18246–18251.

Holty J.E., Kim R.Y., Bravata D.M., (2006). Anthrax: a systematic review of atypical presentations. Ann. Emerg. Med. 48(2),270–280. Review.

Huang, J., Tan, P.H., Li, K.B., Matsumoto, K., Tsujimoto, M., Bay, B.H., 2005. Y-box binding protein, YB-1, as a marker of tumor aggressiveness and response to adjuvant chemotherapy in breast cancer. Int. J. Oncol. 26, 607–613.

Karginov, V.A., Nestorovich, E.M., Moayeri, M., Leppla, S.H., Bezrukov, S.M., 2005. Blocking anthrax lethal toxin at the protective antigen channel by using structure-inspired drug design. Proc. Natl. Acad. Sci. U. S. A. 102 (42), 15075–15080.

Krishnan, A., Li, K.B., Issac, P., 2004. Rapid detection of conserved regions in protein sequences using wavelets. In Silico Biol. 4 (2), 133–148.

Lazovic, J., 1996. Selection of amino acid parameters for Fourier transform-based analysis of proteins. Comput. Appl. Biosci. 16, 553–558.

Lee, J.O., Rieu, P., Arnaout, M.A., Liddington, R., 1995. Crystal structure of the A domain from the alpha subunit of integrin CR3 (CD11b/CD18). Cell 80 (4), 631–638.

Leppla, S.H., 1982. Anthrax toxin edema factor: a bacterial adenylate cyclase that increases cyclicAMP concentrations of eukaryotic cells. Proc. Natl. Acad. Sci. U. S. A. 79, 3162–3166.

Mayer, T.A., Bersoff-Matcha, S., Murphy, C., Earls, J., Harper, S., Pauze, D., Nguyen, M., Rosenthal, J., Cerva Jr., D., Druckenbrod, G., Hanfling, D., Fatteh, N., Napoli, A., Nayyar, A., Berman, E.L., 2001. Clinical presentation of inhalational anthrax following bioterrorism exposure: report of 2 surviving patients. JAMA 286, 2549–2553.

Milne, J.C., Furlong, D., Hanna, P.C., Wall, J.S., Collier, R.J., 1994. Anthrax protective antigen forms oligomers during intoxication of mammalian cells. J. Biol. Chem. 269 (32), 20607–20612.

Mogridge, J., Cunningham, K., Lacy, D.B., Mourez, M., Collier, R.J., 2002. The lethal and edema factors of anthrax toxin bind only to oligomeric forms of the protective antigen. Proc. Natl. Acad. Sci. U. S. A. 99 (10), 7045–7048.

Molloy, S.S., Bresnahan, P.A., Leppla, S.H., Klimpel, K.R., Thomas, G., 1992. Human furin is a calcium-dependent serine endoprotease that recognizes the sequence Arg-X-X-Arg and efficiently cleaves anthrax toxin protective antigen. J. Biol. Chem. 267 (23), 16396–16402.

Mongiat, M., Mungiguerra, G., Bot, S., Mucignat, M.-T., Giacomello, E., Doliana, R., 2000. Self assembly and supramolecular organization of EMILIN (Elastin Microfibril Interface Located proteIN). J. Biol. Chem. 275 (33), 25471–25480.

Mongiat, M., Ligresti, G., Marastoni, S., Lorenzon, E., Doliana, R., Colombatti, A., 2007. Regulation of the extrinsic apoptotic pathway by the extracellular matrix glycoprotein EMILIN2. Mol. Cell Biol. 27 (20), 7176–7187.

Parbhane, R.V., Unniraman, S., Tambe, S.S., Kulkarni, B.D., 2000. Optimum DNA curvature using a hybrid approach involving an artificial neural network and genetic algorithm. J. Biomol. Struct. Dyn. 17, 665–672.

Pham, T.D., 2006. LPC cepstral distortion measure for protein sequence comparison. IEEE Trans. Nanobiosci. 5, 83–88.

Rosovitz, M.J., Schuck, P., Varughese, M., Chopra, A.P., Mehra, V., Singh, Y., McGinnis, L.M., Leppla, S.H., 2003. Alanine-scanning mutations in domain 4 of anthrax toxin protective antigen reveal residues important for binding to the cellular receptor and to a neutralizing monoclonal antibody. J. Biol. Chem. 278 (33), 30936–30944.

Santelli, E., Bankston, L.A., Leppla, S.H., Liddington, R.C., 2004. Crystal structure of a complex between anthrax toxin and its host cell receptor. Nature 430 (7002), 905–908.

Scobie H.M., Young J.A., (2005). Interactions between anthrax toxin receptors and protective antigen. Curr. Opin. Microbiol. 1,1006–1112. Review.

Scobie, H.M., Rainey, G.J., Bradley, K.A., Young, J.A., 2003. Human capillary morphogenesis protein 2 functions as an anthrax toxin receptor. Proc. Natl. Acad. Sci. U. S. A. 100 (9), 5170–5174.

Schenk, P.M., Baumann, S., Mattes, R., Steinbiss, H.H., 1995. Improved high-level expression system for eukaryotic genes in *Escherichia coli* using T7 RNA polymerase and rare ArgtRNAs. Biotechniques 19, 196–200.

Sellman, B.R., Mourez, M., Collier, R.J., 2001. Dominant-negative mutants of a toxin subunit: an approach to therapy of anthrax. Science 292 (5517), 695–697.

Shepherd, A.J., Gorse, D., Thornton, J.M., 2003. A novel approach to the recognition of protein architecture from sequence using Fourier analysis and neural networks. Proteins 50, 290–302.

Singh, Y., Khanna, H., Chopra, A.P., Mehra, V., 2001. A dominant negative mutant of *Bacillus anthracis* protective antigen inhibits anthrax toxin action in vivo. J. Biol. Chem. 276 (25), 22090–22094.

Sinkala, Z., 2006. Soliton/exciton transport in proteins. J. Theor. Biol. 241, 919–927.

Veljkovic, V., 1980. A theoretical approach to preselection of carcinogens and chemical carcinogenesis. Gordon & Breach, New York.

Veljkovic, V., Cosic, I., 1987. A novel method of protein analysis for prediction of biological function: application to tumor toxins. Cancer Biochem. Biophys. 9, 139–148.

Veljkovic, V., Metlas, R., 1998. Identification of nanopeptide from HTLV-III, ARV-2 and LAV envelope gp120 determining binding to T4 cell surface protein. Cancer Biochem. Biophys. 10, 191–206.

Veljkovic, V., Slavic, I., 1972. Simple general-model pseudopotential. Phys. Rev. Lett. 29, 105–107.

Vitale, G., Pellizzari, R., Recchi, C., Napolitani, G., Mock, M., Montecucco, C., 1998. Anthrax lethal factor cleaves the N-terminus of MAPKKS and induces tyrosine/threonine phosphorylation of MAPKS in cultured macrophages. Biochem. Biophys. Res. Commun. 248, 706–711.

Wei, W., Lu, Q., Chaudry, G.J., Leppla, S.H., Cohen, S.N., 2006. The LDL receptor-related protein LRP6 mediates internalization and lethality of anthrax toxin. Cell 124 (6), 1141–1154.

Wen, Z., Wang, K., Li, F., Nie, F., Yang, Y., 2005. Analyzing functional similarity of protein sequences with discrete wavelet transform. Comput. Biol. Chem. 29, 220–228.

Whittaker C.A., Hynes R.O., (2002). Distribution and evolution of von Willebrand/integrin A domains: widely dispersed domains with roles in cell adhesion and elsewhere. Mol. Biol. Cell. 13(10),3369–3387. Review.

Young, J.J., Bromberg-White, J.L., Zylstra, C., Church, J.T., Boguslawski, E., Resau, J.H., Williams, B.O., Duesbery, N.S., 2007. LRP5 and LRP6 are not required for protective antigen-mediated internalization or lethality of anthrax lethal toxin. PLoS Pathog. 3 (3), e27 (March).

Zacchigna, L., Vecchione, C., Notte, A., Cordenonsi, M., Dupont, S., Maretto, S., Cifelli, G., Ferrari, A., Maffei, A., Fabbro, C., Braghetta, P., Marino, G., Selvetella, G., Aretini, A., Colonnese, C., Bettarini, U., Russo, G., Soligo, S., Adorno, M., Bonaldo, P., Volpin, D., Piccolo, S., Lembo, G., Bressan, G.M., 2006. Emilin1 links TGF-beta maturation to blood pressure homeostasis. Cell 124 (5), 893–895.